VOL. 24, NO. 3, 2025, 351-355
elektrika.utm.my
ISSN 0128-4428

ELEKTRIKA
Journal of Electrical Engineering

Non-Orthogonal Multiple Access for Hybrid RIS-UAV-Assisted Communication

Chi Yen Goh[1] and **Chee Yen Leow**[1*]

[1]Wireless Communication Centre, Faculty of Electrical Engineering, Universiti Teknologi Malaysia, 81310 UTM Skudai, Johor, Malaysia.

[*]Corresponding author: bruceleow@utm.my

Abstract: Reconfigurable Intelligent Surfaces (RIS) have gained increasing attention for the ability to manipulate the propagation environment intelligently. When integrated with Unmanned Aerial Vehicles (UAV), forming a RIS-UAV system, the RIS can be deployed flexibly and provide improved coverage, especially in challenging communication environments. In this paper, we focus on a hybrid RIS-UAV system that combines both passive and active elements to improve the system performance. The achievable rate performance of the hybrid RIS-UAV system is investigated under two cooperative Non-Orthogonal Multiple Access (NOMA) transmission schemes: a conventional NOMA scheme with fixed power allocation based on user channel conditions, and a cognitive radio-inspired NOMA (CR-NOMA) scheme where power allocation prioritized the Quality-of-Service (QoS) requirements of the primary user. The achievable rate performance is analyzed through extensive Monte Carlo simulations. The results demonstrate that dynamic power allocation in CR-NOMA significantly outperforms the fixed power allocation in conventional NOMA, showcasing the potential of hybrid RIS-UAV system for serving multiple users with adaptive power allocation.

Keywords: Multiuser Communication, Non-Orthogonal Multiple Access, Reconfigurable Intelligent Surfaces, Unmanned Aerial Vehicles

Article History: received 6 May 2025; accepted 2 July 2025; published 22 December 2025
Digital Object Identifier 10.11113/elektrika.v24n3.741

1. INTRODUCTION

Reconfigurable Intelligent Surfaces (RIS) have gained significant attention as a transformative technology for the sixth generation (6G) wireless networks. By intelligently adjusting the phase shifts or amplitude of the incident electromagnetic waves through a surface composed of a large number of low-cost reflecting elements, RIS can enhance the signal strength, and improve the reliability of the communication link [1]. Unlike conventional relays that require radio frequency (RF) chains for signal processing, RIS reflect incoming signals without RF chains, resulting in significantly lower power consumption and hardware complexity [2].

To further enhance the flexibility and adaptability of RIS-enabled systems, recent research has explored the integration of Unmanned Aerial Vehicles (UAV) with RIS. The aerial deployment of RIS, known as RIS-UAV, enables dynamic positioning of RIS in three-dimensional (3D) space to establish stronger line-of-sight connections with the ground nodes, avoid physical obstructions, and provide coverage in underserved areas [3]. RIS-UAV is particularly advantageous in disaster recovery operations, remote regions, and dense urban environments where ground-based RIS is inadequate or impractical.

Building upon the advantages of RIS-UAV, incorporating non-orthogonal multiple access (NOMA) further enhances the system capability. NOMA is one of the key enabling technologies for the fifth-generation (5G) wireless network that enhances spectral efficiency by allowing multiple users to share the resources at the same time or same frequency. Unlike traditional orthogonal multiple access (OMA) that allocate different orthogonal resources to each user, NOMA superimposes the signals in power or code domain, thus improving spectral efficiency, allowing massive connectivity, and ensuring the diverse quality-of-service (QoS) of the users [4].

Recent studies have investigated the integration of RIS-UAV to enable NOMA transmission for serving multiple users [5], [6]. In these studies, the RIS-UAV operates in a purely passive mode, reflecting incident signals without amplification. While passive RIS-UAV offers significant energy and cost advantages, their performance is inherently limited by the absence of active signal processing, particularly when the reflected signals experience severe path loss or when users are located far from the RIS-UAV [7]. To overcome these limitations, emerging research has investigated active and hybrid RIS-UAV architectures. A hybrid RIS combines both passive and active reflecting elements, where the active elements are equipped with low-power amplifiers capable of boosting the reflected signal. Compared to fully active and fully passive RIS-UAV, hybrid RIS-UAV strikes a balance between energy efficiency and signal enhancement [8], [9].

To further understand the potential of hybrid RIS-UAV systems, this paper investigates their performance under two representative cooperative NOMA transmission schemes. First, we consider conventional NOMA, where users are paired based on their channel conditions, and power is statically allocated such that the user with the weaker channel receives more power, while the user with the stronger channel receives less power. Second, we examine cognitive radio-inspired NOMA (CR-NOMA), in which one user is designated as the primary user and is guaranteed a minimum QoS, such as a data rate equal to that achievable under OMA or a predefined threshold. The remaining power is then allocated to the secondary user, only if the primary user's requirement is satisfied. The sum-rate performance of hybrid RIS-UAV system under both NOMA schemes is analytically derived, and simulations are performed. The results, presented in the following sections, provide new insight into the effectiveness of hybrid RIS-UAV in enhancing multiuser communication performance under different cooperative NOMA paradigms.

2. SYSTEM MODEL

We consider a downlink cooperative NOMA system where a hybrid RIS is mounted on a UAV to facilitate communication between a single-antenna base station (BS) and two single-antenna users, as shown in Figure 1. All nodes are assumed to be static except the hybrid RIS-UAV, which serves as a mobile aerial relay. In this setup, only User 1 is assisted by the hybrid RIS-UAV due to the absence of a direct link with the BS, while the User 2 communicates directly with the BS without RIS-UAV assistance.

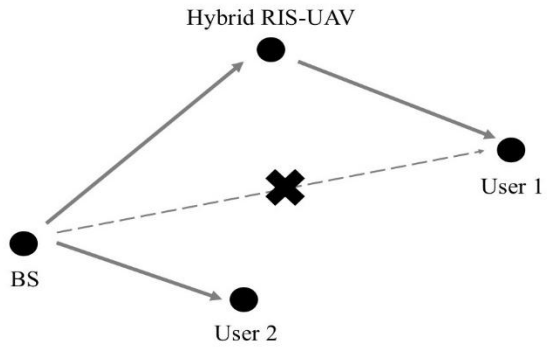

Figure 1. Hybrid RIS-UAV-enabled cooperative NOMA system.

2.1 Conventional NOMA Scheme and Channel Model

In the conventional NOMA scheme, both users are served simultaneously by superimposing their signals with different power levels at the BS. User 1, which suffers from a blocked direct link to the BS, is supported via the hybrid RIS-UAV. User 2, has a strong direct link and receives its signal only from the BS.

Let $h_2 \in \mathbb{C}$ denote the complex channel coefficient between the BS and User 2. For User 1, the effective channel consists of the cascaded BS-RIS-User 1 link. Let $\mathbf{h}_{r,1} \in \mathbb{C}^{N\times 1}$ and $\mathbf{h}_{b,r} \in \mathbb{C}^{1\times N}$ represent the channels from the hybrid RIS-UAV to User 1 and from the BS to the hybrid RIS-UAV, respectively, with N total reflecting element of the hybrid RIS-UAV. As presented in [8], the reflection matrix of the hybrid RIS is denoted by $\boldsymbol{\Theta} = \text{diag}(\theta_1, \ldots, \theta_N)$, where each element is defined as $\theta_n = \beta_n e^{j\phi_n}$, with the phase shift $\phi_n \in (0, 2\pi)$ and amplitude

$$\beta_n^2 = \frac{P_r}{N_a\left(P_b h_{b,r}+\sigma^2\right)}, \tag{1}$$

where P_r is the RIS transmit power, N_a is the number of active RIS elements, P_b is the BS transmit power, and σ^2 is the noise power at the hybrid RIS-UAV. Equation (1) is only valid for the active element and $\beta_n = 1$ for passive element. Therefore, the effective cascade channel for User 1 is expressed as

$$h_1 = \mathbf{h}_{r,1}\boldsymbol{\Theta}\mathbf{h}_{b,r}. \tag{2}$$

According to [4], the base station transmits the superimposed signal

$$x = \sqrt{a_1 P_b}s_1 + \sqrt{a_2 P_b}s_2, \tag{3}$$

where s_1 and s_2 are the information symbols for the Users 1 and 2, respectively, and $a_1, a_2 \in (0,1)$ are the power allocation coefficients with $a_1 + a_2 = 1$, and typically $a_1 > a_2$ to favor the weak user.

The received signals at the two users are given as

$$y_1 = h_1 x + n_1, \;\; y_2 = h_2 x + n_2, \tag{4}$$

where n_1 and n_2 are zero-mean complex Gaussian noise terms with variance σ^2.

For User 1 that assisted by the hybrid RIS-UAV, the received signal contains both its designated signal and the interference from the User 2's signal. Following the conventional NOMA formulation in [4], the signal-to-interference-plus-noise ratio (SINR) at User 1 is given as

$$\gamma_1 = \frac{a_1 P_b |h_1|^2}{a_2 P_b |h_1|^2 + \sigma^2 |h_{r,1}\boldsymbol{\Theta}|^2 + \sigma^2}, \tag{5}$$

since User 1 directly detects its intended signal while treating User 2's signal as noise. For User 2, successive interference cancellation (SIC) technique is applied. Specifically, User 2 first decodes the signal intended for User 1 while treating its own signal as interference. The SINR at User 2 when decoding User 1's signal during the SIC process is given as

$$\gamma_{2\to 1} = \frac{a_1 P_b |h_2|^2}{a_2 P_b |h_2|^2 + \sigma^2}. \tag{6}$$

Upon successfully decoding and removing User 1's signal, User 2 then decodes its own signal. The SINR at User 2 for decoding its own signal without interference is

$$\gamma_2 = \frac{a_2 P_b |h_2|^2}{\sigma^2}. \tag{7}$$

Therefore, the achievable sum-rate is the combination of

the achievable rate of Users 1 and 2, which is expressed as

$$R_t = \log_2(1 + \min\{\gamma_1, \gamma_{2\to1}\}) + \log_2(1 + \gamma_2). \quad (8)$$

2.2 Cognitive Radio-Inspired NOMA

In the CR-NOMA scheme, the BS designates User 1 as the primary user, whose QoS requirement must be guaranteed. User 2, which has a strong direct link to the BS, acts as the secondary user, and is allowed to share the spectrum only if the QoS of the primary user is met. Let $R_{1,min}$ denotes the minimum rate requirement for User 1, and the achievable rate of User 1 must be greater or equal to the minimum rate requirement, which is expressed as

$$\log_2\left(1 + \frac{a_1 P_b |h_1|^2}{a_2 P_b |h_1|^2 + \sigma^2 |h_{r,1}\boldsymbol{\Theta}|^2 + \sigma^2}\right) \geq R_{1,min}. \quad (9)$$

Therefore, the minimum required power allocation for the User 1, a_1 is given as

$$a_1 \geq \frac{\left(2^{R_{1,min}} - 1\right)\left(a_2 P_b |h_1|^2 + \sigma^2 |h_{r,1}\boldsymbol{\Theta}|^2 + \sigma^2\right)}{P_b |h_1|^2}. \quad (10)$$

Once the system allocates the minimum a_1 for the User 1, the remaining power $a_2 = 1 - a_1$ is allocated to the User 2. It is important to note that the resulting SINR and achievable rate expressions for both users in CR-NOMA scheme remain the same as those in conventional NOMA, as given in Equations (5) - (7). Accordingly, the sum-rate expression of CR-NOMA scheme also follows the same form as conventional NOMA, as given in Equation (8). The key difference lies in the power allocation strategy, in which the power allocation mechanism in CR-NOMA scheme is governed by the QoS constraint of the User 1 while conventional NOMA is governed purely by the channel conditions.

3. RESULTS AND DISCUSSIONS

To evaluate the system performance, Monte Carlo simulations are conducted with over 100,000 independent channel realizations. The channels from the BS to the hybrid RIS-UAV, from hybrid RIS-UAV to the User 1, and from the BS to the User 2 are modeled using the Al-Hourani probabilistic path loss model with the Rayleigh small-scale fading [8], [10]. Unless stated otherwise, $N = 200$, $N_a = 1$, $\sigma^2 = -80$ dBm, $P_b = 10$ dBm, and $P_r = 5$ dBm. The BS is positioned at the origin (0, 0, 0), the hybrid RIS-UAV hovers at (120, 10, 100), User 1 is located at (250, 40, 0) and User 2 is located at (20, 0, 0).

The comparative analysis of the simulation results for conventional NOMA, OMA, and two CR-NOMA configurations, denoted as CRNOMA-1 and CRNOMA-2, are presented as shown in Figures 2 to 5. In CRNOMA-1, the power allocation is constrained such that the primary user (User 1) achieves a rate equal to its OMA counterpart. Meanwhile, CRNOMA-2 ensures a target rate constraint of 1 bps/Hz for the primary user, allowing the remaining power to be allocated to the secondary user (User 2).

Figure 2 illustrates the power allocation coefficients across all NOMA configurations. For the conventional NOMA scheme, power allocation is fixed based on channel conditions, where more power is assigned to the weak user (User 1) to be consistent with the standard NOMA principle. In CRNOMA-1, power allocation to User 1 is dynamically adjusted to meet the rate requirement as the OMA scheme. At lower transmit power levels of BS, User 2 receives a larger share of power since User 1 can still achieve its OMA rate with a smaller allocation due to lower interference. However, as the transmit power increases, User 1 requires more power to maintain its OMA rate in the presence of higher interference. In CRNOMA-2, a minimum rate requirement of 0.5 bps/Hz is set for User 1. Consequently, at lower transmit power, a larger portion of power is allocated to User 1 to meet its QoS requirement. Once this constraint is satisfied, any additional power is directed toward User 2, hence more power is allocated to the User 2 as the transmit power of BS increases.

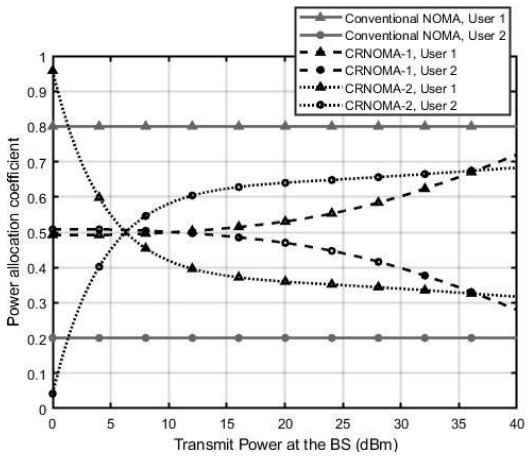

Figure 2. Power allocation coefficients across different NOMA configurations

Figure 3 depicts the achievable rate of User 1 across different schemes. As expected, CRNOMA-1 consistently achieves the same rate as OMA for User 1. The conventional NOMA scheme exhibits a higher rate than OMA, attributed to the relatively larger power allocation given to the User 1. Besides, the rate for User 1 in CRNOMA-2 is maintained as the minimum rate constraint is met.

The achievable rate for User 2 is shown in Figure 4. Among all schemes, CRNOMA-2 yields the highest rate for User 2, as it benefits from the excess power not required by User 1 to meet its QoS requirement. The same theory applied to the CRNOMA-1 scheme that benefits from the excess power not required by User 1 to meet its OMA-equivalent rate. At lower transmit power of BS, conventional NOMA has a lower rate for User 2 than the OMA scheme because less power is allocated to the User 2. As the transmit power increases, conventional NOMA outperforms OMA scheme due to the sharing of spectrum, even the power allocation coefficient for User 2 is still lower than OMA cases.

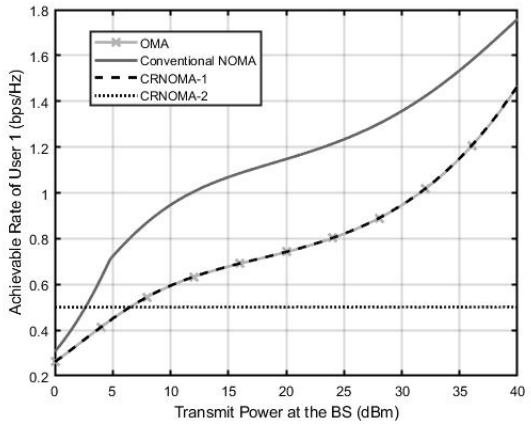

Figure 3. Achievable rate of User 1 across different multiple access configurations.

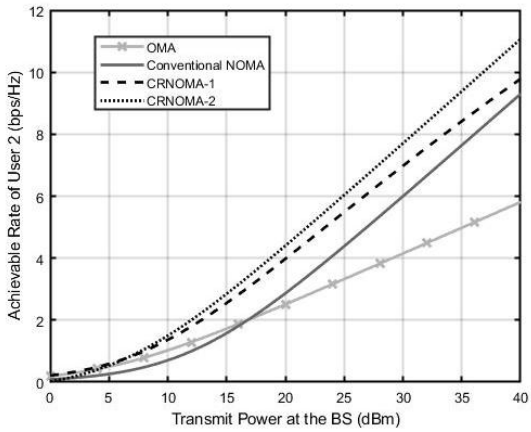

Figure 4. Achievable rate of User 2 across different multiple access configurations.

Figure 5 presents the overall achievable sum rate of the system under each configuration. The sum rate trend is similar to that of User 2's rate (Figure 4). This is because User 2 is positioned closer to the BS, so it generally achieves higher rate than User 1 and thus dominates the sum rate. CRNOMA-2 achieves the highest sum rate among all schemes, balancing the QoS of the User 1 while maximizing the rate for User 2. In addition, conventional NOMA achieves a higher sum rate than OMA scheme due to the efficient spectrum sharing.

4. CONCLUSION

In conclusion, this paper presented a performance comparison of a hybrid RIS-UAV-assisted system under different cooperative NOMA configurations. The simulation results show that fixed-power conventional NOMA offers limited sum-rate performance, while CR-NOMA schemes achieve superior sum-rate performance with power allocation adapting to the User's QoS requirements. These findings demonstrate the benefits of combining hybrid RIS-UAV with dynamic multiple access strategies to serve multiple users. As a direction for future work, the integration of UAV trajectory optimization and real-time power allocation could be explored to further maximize the achievable sum rate in dynamic communication environments.

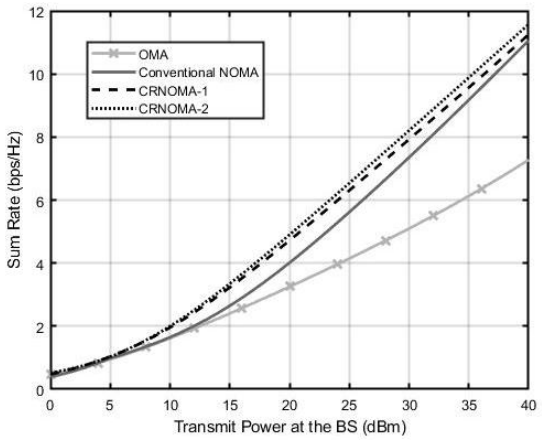

Figure 5. Sum rate performance across different multiple access configurations

ACKNOWLEDGMENT

This work was supported by the Ministry of Higher Education Malaysia through the Higher Institution Centre of Excellence (HICOE) Grant 4J636 and in part by EU HORIZON MSCA-SE project TRACE-V2X under Grant Agreement No. 101131204.

REFERENCES

[1] Q. Wu, S. Zhang, B. Zheng, C. You, and R. Zhang, "Intelligent reflecting surface-aided wireless communications: A tutorial," *IEEE Trans. Commun.*, vol. 69, pp. 3313–3351, 2021.

[2] X. Pang, M. Sheng, N. Zhao, J. Tang, D. Niyato, and K. Wong, "When UAV meets IRS: expanding air-ground networks via passive reflection," *IEEE Wirel. Commun.*, vol. 28, no. 5, pp. 164–170, 2021.

[3] K.-W. Park, H. M. Kim, and O.-S. Shin, "A survey on intelligent reflecting-surface-assisted uav communications," *Energies*, vol. 15, no. 14, p. 5143, Jul 2022.

[4] L. Dai, B. Wang, Z. Ding, Z. Wang, S. Chen, and L. Hanzo, "A survey of non orthogonal multiple access for 5g," *IEEE Commun. Surv. Tutorials*, vol. 20, no. 3, pp. 2294–2323, 2018.

[5] S. K. Singh, K. Agrawal, K. Singh, C. Li, and Z. Ding, ''Noma enhanced hybrid RIS-UAV-assisted full-duplex communication system with imperfect SIC and CSI,'' *IEEE Trans. Commun.*, vol. 70, pp. 7609-7627, 2022.

[6] D. Wang, Y. Zhao, Y. Lou, L. Pang, Y. He and D. Zhang, ''Secure noma based RIS-UAV networks: passive beamforming and location optimization,'' *IEEE Global Commun. Conf.*, Rio de Janeiro, Brazil, pp. 3168-3173, 2022.

[7] C. Y. Goh and C. Y. Leow, "A comparative study of reconfigurable intelligent surfaces with relays in UAV cooperative communications," in *Advances in Information and Communication*, vol. 1. Berlin, Germany: Springer, pp. 100–106, 2023.

[8] C. Y. Goh, C. Y. Leow, and R. Nordin, ‘‘Energy efficiency of unmanned aerial vehicle with reconfigurable intelligent surfaces: a comparative study,” *Drones*, vol. 7, no. 2, pp. 98, 2023.

[9] C. Y. Goh, C.Y. Leow, C. H. Foh, I. Orikumhi, S. Kim and J. Wu, ‘‘Energy efficient relay for unmanned aerial vehicle with onboard hybrid reconfigurable intelligent surfaces,’’ *ICC 2024-IEEE Int. Conf. Commun.*, Denver, CO, USA, pp. 3452-3457, 2024.

[10] A. Al-Hourani, S. Kandeepan, and S. Lardner, “Optimal lap altitude for maximum coverage,” *IEEE Wireless Commun. Lett.*, vol. 3, pp. 569– 572, 2014.